Print ISSN : 0022-2755
Journal of Mines, Metals and Fuels
Contents available at: www.informaticsjournals.com/index.php/jmmf

Local Thermal Non-Equilibrium Dominant Darcy-Rayleigh-Benard-Magneto-Marangoni Convection in a Composite Layer

R. Sumithra[1] and Shyamala Venkatraman[2*]

[1]Associate Professor and [2]Research Scholar, Department of UG, PG Studies & Research in Mathematics, Government Science College Autonomous, Nrupathunga University, Bengaluru, Karnataka, India sumitra_diya@yahoo.com and svr02009@gmail.com

Abstract

The domination by Local Thermal Non-Equilibrium (LTNE) with regard to the onset of Darcy-Rayleigh-Benard-Marangoni (DRBM) convection swayed by magnetic field in a composite layer set-up is studied pertinent to incompressible fluid. The precinct above the fluid layer is presumed to be free and that below the porous layer is presumed to be rigid. Regular perturbation technique is exercised on the acquired problem to achieve the analytical solution taking adiabatic-adiabatic conditions into account at the boundaries. Effects of parameters such as solid phase thermal expansion ratio, solid phase thermal diffusivity ratio and inter-phase thermal diffusivity ratio that influences LTNE are discussed. The impact of change in measures of variables viz. fluid phase thermal expansion ratio, fluid phase thermal diffusivity ratio, porous parameter, thermal ratio, Chandrasekhar number and Marangoni number with respect to both LTNE and LTE situations are together explored and portrayed graphically. It is to be noted that for smaller values of fluid phase thermal expansion ratio and fluid phase thermal diffusivity ratio, the LTNE effects are prominent and cannot be ignored.

Keywords: *Marangoni convection, local thermal non-equilibrium (LTNE), composite layer, regular perturbation technique, magnetic field, chandrasekhar number*

Nomenclature:

English letters			
$\vec{q}_{fl} = (u_{fl}, v_{fl}, w_{fl})$	: velocity vector	C_p	: specific heat capacity
t	: time	Q_{fl}, Q_{po}	: Chandrasekhar numbers, defined below
P_{fl} & P_{po}	: pressure	h	: inter-phase heat transfer coefficient
g	: acceleration due to gravity	a_{fl} & a_{po}	: non dimensional horizontal wave numbers
T_{fl}, T_{fpo} & T_{spo}	: temperatures		
T_0	: interface temperature		
K	: permeability		

*Corresponding author

English letters			
n_{fl} & n_{po}	: frequencies	H	: scaled inter-phase heat transfer coefficient
W_{fl} & W_{po}	: dimensionless vertical velocities	$\hat{T}$	: thermal ratio
R_{fl}, R_{Tfpo}, R_{Tspo}	: Rayleigh numbers, defined below	$\hat{d}$	: depth ratio
Greek Symbols			
ρ_0	: referrence density	κ_{FTD} & κ_{STD}	: thermal diffusivity ratio
μ_{fl}	: fluid viscosity	β	: porous parameter
ρ_{fl} & ρ_{po}	: fluid density	β^2	: Darcy number
κ_{fl}, κ_{fpo} & κ_{spo}	: thermal diffusivities	τ	: inter-phase thermal diffusivity ratio
α_{Tfl}, α_{Tfpo} & T_{spo}	: thermal expansion coefficients	τ_{fpo} & τ_{mpo}	: diffusivity ratios
ϕ	: porosity	$\hat{\mu}$	: viscosity ratio
α_{FTE} & α_{STE}	: thermal expansion ratio		
Subscripts			
fl	: fluid layer	s	: solid phase
po	: porous medium	b	: basic state
f	: fluid phase		

1. Introduction

Problems involving heat transport via porous environs has been captivating researchers substantially in the existing circumstances to cope up with the persisting demand in engineering and industrial domains. Such problems drew attention to the pair of models viz. Local Thermal Non-Equilibrium (LTNE) model and Local Thermal Equilibrium (LTE) model. The process of heat flow through a porous medium is modelled under Local Thermal Equilibrium conditions when disparity in temperature between the fluid and the solid phases diminishes and under Local Thermal Non-Equilibrium conditions with the enhancing thermal disparity. LTNE modelling booms up by the occurrence of transitional convective heat transfer coefficient. Processes like cooling of electronic gadgets, geothermal structure etc. deal with metal foams having tremendous pores, sand and gravel and such other porous substances. Diverse industries such as crystal growth under hydrothermal conditions, storage of energy etc. tackle the convective heat transfer problems in their thermic structure with an aid of distinct means of magnetic field since magnetic field can undeniably manipulate the two processes of heat transmission and cooling.

Min Zeng et al [2007] examined natural convection in a porous medium filled system influenced by magnetic field in the presence of local thermal non-equilibrium and they performed the same for diamagnetic fluid in [2009]. Phadungsak & Waraporn [2012] studied the effect of electromagnetic energy on natural convection numerically in a porous set-up with respect to local thermal non-equilibrium. Srivastava & Bhadauria [2016] analysed the instability of fingering in case of a porous system taking cross-diffusion effect into account in the presence of magnetic field for a local thermal non-equilibrium model. Zargartalebi et al [2016] investigated the influence of local thermal non-equilibrium on natural convection in a porous enclosure comprising of nanofluid for Buongiorno's model. Mehryan et al [2018] studied conjugate natural convection in a porous enclosure composed of micropolar nanofluid under local thermal non-equilibrium conditions. Jyoti [2019] examined the impact of magnetic field on nanofluid under local thermal non-equilibrium conditions. Mohsen et al

[2019] investigated the natural convection within a porous medium subjected to non-uniform magnetic field in a local thermal non-equilibrium set-up. Ravisha et al [2019] studied the Cattaneo effect on the onset of convection in a porous media saturated with ferrofluid influenced by local thermal non-equilibrium. Mohsen [2019] analysed the attributes of heat and mass flow in a porous media consisting of nanofluid under local thermal non-equilibrium and local thermal equilibrium conditions with respect to Darcy model as well as Brinkman model. Pouya et al [2020] examined mixed thermomagnetic convection with regard to local thermal equilibrium as well as local thermal non-equilibrium conditions in a porous cavity comprising ferrofuid using rotating cylinders. Puneet & Meenakshi [2020] analysed the impact of local thermal non-equilibrium on a rotating layer of Newtonian fluid in the presence of heat source together with magnetic field. Sumithra & Manjunatha [2020] studied the impact of magnetic field on Darcy-Benard-Marangoni convection in a composite layer with adiabatic boundaries in the presence of heat source/sink as well as non-uniform temperature gradients.

Impelled by the aforementioned review of literatures, this paper intends on onset of Darcy-Rayleigh-Benard-Marangoni (DRBM) convection controlled by magnetic field in a composite layer set-up bearing rigid-free boundaries. Effects of parameters such as solid phase thermal expansion ratio, solid phase thermal diffusivity ratio and inter-phase thermal diffusivity ratio that influences LTNE are studied. The change in measures of variables viz. fluid phase thermal expansion ratio, fluid phase thermal diffusivity ratio, porous parameter, thermal ratio, Chandrasekhar number and Marangoni number with respect to both LTNE and LTE situations are together explored and portrayed graphically.

2.0 Mathematical formulation

An infinite horizontal layer involving incompressible, Boussinesq electrically conducting fluid holding thickness d_{fl} is considered. Densely packed porous layer saturated with same fluid with thickness d_{po} lies beneath the fluid layer levied with magnetic field of intensity H_0 in the perpendicular z-direction. The precinct below the porous layer is presumed to be rigid and that above the fluid layer is presumed to be with surface tension effects based on temperature. A Cartesian coordinate system in which the origin is placed at the interface between fluid and porous layers and the z-axis pointing upright is considered. For the porous layer, solid phase as well as the fluid phase are purported to be in LTNE and a solid-fluid field model is considered to express distinctly the temperatures with regard to the solid and fluid phases. The above system is governed by the following basic equations.

$$\nabla.\vec{q}_{fl} = 0 \quad \text{... (1)}$$

$$\nabla.\overrightarrow{H_{fl}} = 0 \quad \text{... (2)}$$

$$\rho_0\left[\frac{\partial \vec{q}_{fl}}{\partial t} + \left(\vec{q}_{fl}.\nabla\right)\vec{q}_{fl}\right] = -\nabla P_{fl} + \mu\nabla^2\vec{q}_{fl} - \rho_{fl}g\hat{k} + \mu_p\left(\overrightarrow{H_{fl}}.\nabla\right)\overrightarrow{H_{fl}} \quad \text{... (3)}$$

$$\frac{\partial T_{fl}}{\partial t} + (\vec{q}_{fl}.\nabla)T_{fl} = \kappa_{fl}\nabla^2 T_{fl} \quad \text{... (4)}$$

$$\frac{\partial \overrightarrow{H_{fl}}}{\partial t} = \nabla\times q_{fl}\times\overrightarrow{H_{fl}} + \nu_m\nabla^2\overrightarrow{H_{fl}} \quad \text{... (5)}$$

$$\rho_{fl} = \rho_0[1-\alpha_{Tfl}(T_{fl}-T_0)] \quad \text{... (6)}$$

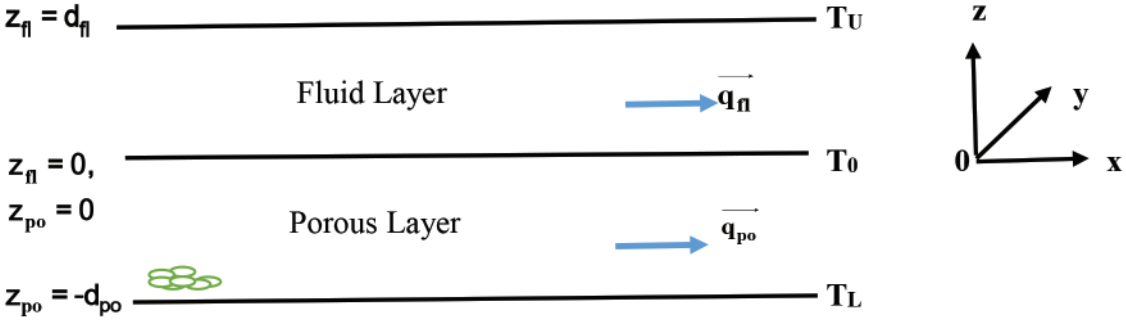

Figure.1. Prototypical Sketch

$$\nabla_{po}.\vec{q}_{po}=0 \quad \text{... (7)}$$

$$\nabla_{po}.\overrightarrow{H_{fl}}=0 \quad \text{... (8)}$$

$$\rho_0\left[\frac{1}{\phi}\frac{\partial\vec{q}_{po}}{\partial t_{po}}+\frac{1}{\phi^2}(\vec{q}_{po}.\nabla_{po})\vec{q}_{po}\right]=-\nabla_{po}P_{po}-\frac{\mu}{K}\vec{q}_{po}-\rho_{po}g\hat{k}+\mu_p\left(\overrightarrow{H_{fl}}.\nabla\right)\overrightarrow{H_{fl}} \quad \text{... (9)}$$

$$(\rho C_p)_{fpo}\left[\phi\frac{\partial T_{fpo}}{\partial t_{po}}+(\vec{q}_{po}.\nabla_{po})T_{fpo}\right]=\phi\kappa_{fpo}\nabla_{po}^{2}T_{fpo}+h(T_{spo}-T_{fpo}) \quad \text{... (10)}$$

$$(1-\phi)(\rho C_p)_{spo}\frac{\partial T_{spo}}{\partial t_{po}}=(1-\phi)\kappa_{spo}\nabla_{po}^{2}T_{spo}-h(T_{spo}-T_{fpo}) \quad \text{... (11)}$$

$$\phi\frac{\partial\overrightarrow{H_{fl}}}{\partial t_{po}}=\nabla_{po}\times q_{po}\times\overrightarrow{H_{fl}}+\nu_{em}\nabla_{po}^{2}\overrightarrow{H_{fl}} \quad \text{... (12)}$$

$$\rho_{po}=\rho_0[1-\alpha_{Tfpo}(T_{fpo}-T_0)-\alpha_{Tspo}(T_{spo}-T_0)] \quad \text{... (13)}$$

The system is quiescent for which the basic state is expressed by

and $[u_{po},v_{po},w_{po},P_{po},T_{fpo},T_{spo}.\overrightarrow{H_{fl}}]=[0,0,0,P_{pob}(z_{po}),T_{fpob}(z_{po}),T_{spob}(z_{po}),H_0(z_{po})]$ ... (15)

in the porous layer

The basic state temperature distributions $T_{flb}(z_{fl})$, $T_{fpob}(z_{po})$ and $T_{spob}(z_{po})$ respectively are found to be

$$T_{flb}(z_{fl})=T_0-\frac{T_0-T_U}{d_{fl}}z_{fl}\ \text{in}\ 0\le z_{fl}\le d_{fl} \quad \text{... (16)}$$

$$T_{fpob}(z_{po})=T_0-\frac{T_L-T_0}{d_{po}}z_{po}=T_{pob}(z_{po})\ \text{in}\ -d_{po}\le z_{po}\le 0 \quad \text{... (17)}$$

For investigating stability of the basic solution, following diminutive disturbances are introduced.

$$[\vec{q}_{fl},P_{fl},T_{fl},\overrightarrow{H_{fl}}]=[0,P_{flb}(z_{fl}),T_{flb}(z_{fl}),H_0(z_{fl})]+[\vec{q}_{fl}',P_{fl}',\theta_{fl},\overrightarrow{H_{fl}}'] \quad \text{... (18)}$$

$$[\vec{q}_{po},P_{po},T_{fpo},T_{spo},\overrightarrow{H_{fl}}]=[0,P_{pob}(z_{po}),T_{fpob}(z_{po}),T_{spob}(z_{po}),H_0(z_{po})]+[\vec{q}_{po}',P_{po}',\theta_{fpo},\theta_{spo}.\overrightarrow{H_{fl}}'] \quad \text{... (19)}$$

where the prime indicates perturbation over the equilibirium counterparts. Now (18) and (19) are placed in the corresponding physical quantities of equations (1) to (13) and are linearized in the customary manner. Then, the pressure term is removed from (3) and (9) by the procedure of operating curl two times on these two equations and keeping only the vertical component.

Next, the resulting equations are nondimensionalised applying $d_{fl},\frac{d_{fl}^{2}}{\kappa_{fl}},\frac{\kappa_{fl}}{d_{fl}},T_0-T_U,H_0$ as the units of length, time, velocity, temperature and magnetic field in the fluid layer correspondingly and $\frac{d_{po}^{2}}{\kappa_{fpo}},\frac{\kappa_{fpo}}{d_{po}},T_L-T_0,H_0$ as the units of time, velocity and temperature in the porous layer whereas the scale for length in the porous layer is $(x_{po},y_{po},z_{po})=d_{po}(x'_{po},y'_{po},z'_{po}-1)$. Following this fashion, the flow- fields pertaining to fluid as well as porous layers can be achieved for all depth ratios $\hat{d}=\frac{d_{po}}{d_{fl}}$. Normal mode analysis is performed on the dimensionless equations as follows:

$$\begin{bmatrix} W_{fl} \\ \theta_{fl} \\ H_{fl} \end{bmatrix} = \begin{bmatrix} W_{fl}(z_{fl}) \\ \theta_{fl}(z_{fl}) \\ H_{fl}(z_{fl}) \end{bmatrix} f_{fl}(x_{fl}, y_{fl}) e^{n_{fl} t} \quad \text{... (20)}$$

$$\begin{bmatrix} W_{po} \\ \theta_{fpo} \\ \theta_{spo} \\ H_{fl} \end{bmatrix} = \begin{bmatrix} W_{po}(z_{po}) \\ \theta_{fpo}(z_{po}) \\ \theta_{spo}(z_{po}) \\ H_{fl}(z_{po}) \end{bmatrix} f_{po}(x_{po}, y_{po}) e^{n_{po} t} \quad \text{... (21)}$$

with $\nabla^2 f_{fl} + a_{fl}^2 f_{fl} = 0$ and $\nabla_{po}^2 f_{po} + a_{po}^2 f_{po} = 0$

The resulting equations are:

in $\mathbf{0 \le Z_{fl} \le 1}$

$$(D_{fl}^2 - a_{fl}^2)^2 W_{fl} = R_{fl} a_{fl}^2 \theta_{fl} + Q_{fl} D_{fl}^2 W_{fl} \quad \text{... (22)}$$

$$(D_{fl}^2 - a_{fl}^2)\theta_{fl} + W_{fl} = 0 \quad \text{... (23)}$$

in $\mathbf{0 \le Z_{po} \le 1}$

$$(D_{po}^2 - a_{po}^2)^2 W_{po} = -\beta^2 R_{Tfpo} a_{po}^2 \theta_{fpo} - \beta^2 R_{Tspo} a_{po}^2 \theta_{spo} \tau - Q_{po} \beta^2 D_{po}^2 W_{po} \quad \text{... (24)}$$

$$\phi(D_{po}^2 - a_{po}^2)\theta_{fpo} + W_{po} = -H(\theta_{spo} - \theta_{fpo}) \quad \text{... (25)}$$

$$(1-\phi)(D_{po}^2 - a_{po}^2)\theta_{spo} = H(\theta_{spo} - \theta_{fpo}) \quad \text{... (26)}$$

Where for the fluid layer, $R_{fl} = \dfrac{g\alpha_{Tfl}(T_0 - T_U)d_{fl}^3}{\nu_{fl}\kappa_{fl}}$ specifies the Rayleigh number, which is thestability criterion for the system, $Q_{fl} = \dfrac{\mu_p H_0^2 d_{fl}^2}{\mu_{fl}\kappa_{fl}\tau_{fpo}}$ specifies the Chandrasekhar number, which denotes the strength of magnetic field, $\tau_{fpo} = \dfrac{\nu_{pov}}{\kappa_{fl}}$ specifies the diffusivity ratio, and for the porous layer, $R_{Tfpo} = \dfrac{g\alpha_{Tfpo}(T_L - T_0)d_{po}^3}{\nu_{fl}\kappa_{fpo}}$ specifies the solid Rayleigh number, $R_{Tspo} = \dfrac{g\alpha_{Tspo}(T_L - T_0)d_{po}^3}{\nu\kappa_{spo}}$ specifies the solid Rayleigh number, $\beta^2 = \dfrac{K}{d_{po}^2} = Da$ specifies the Darcy number, $Q_{po} = \dfrac{\mu_p H_0^2 d_{po}^2}{\mu_{fl}\kappa_{po}\tau_{mpo}} = Q_{fl}\varepsilon\hat{d}^2$ specifies the Chandrasekhar number, $\tau_{mpo} = \dfrac{\nu_{epo}}{\kappa_{po}}$ specifies the diffusivity ratio, $\tau = \dfrac{\kappa_{spo}}{\kappa_{fpo}}$ specifies the ratio of thermal diffusivity of the solid to the fluid phase, $H = \dfrac{hd_{po}^2}{\kappa_{fpo}}$ specifies the scaled inter-phase heat transfer coefficient.

Equations (22) to (26) are ordinary differential equations of fourteenth order and required to be solved with the help of the following fourteen boundary conditions.

3. Boundary conditions

Normal mode expansion performed on the appropriate boundary conditions after non dimensionalization. They are,

$$W_{fl}(1)=0,\ D_{fl}{}^2W_{fl}(1)+M_{fl}a_{fl}{}^2\theta_{fl}(1)=0,\ D_{fl}\theta_{fl}(1)=0,$$

$$\hat{T}W_{fl}(0)=W_{po}(1),\quad \hat{T}\hat{d}D_{fl}W_{fl}(0)=\hat{\mu}D_{po}W_{po}(1)$$

$$\theta_{fl}(0)=\hat{T}\theta_{fpo}(1),\quad \theta_{fl}(0)=\hat{T}\theta_{spo}(1),\quad D_{fl}\theta_{fl}(0)=D_{po}\theta_{fpo}(1),\quad D_{fl}\theta_{fl}(0)=D_{po}\theta_{spo}(1)$$

$$\hat{T}\hat{d}^3\beta^2[D_{fl}{}^3W_{fl}(0)-3a_{fl}{}^2D_{fl}W_{fl}(0)]=-D_{po}W_{po}(1)+\hat{\mu}\beta^2[D_{po}{}^3W_{po}(1)-3a_{po}{}^2D_{po}W_{po}(1)]$$

$$\hat{T}\hat{d}^2(D_{fl}{}^2+a_{fl}{}^2)W_{fl}(0)=\hat{\mu}(D_{po}{}^2+a_{po}{}^2)W_{po}(1)$$

$$W_{po}(0)=0,\quad D_{po}W_{po}(0)=0,\quad D_{po}\theta_{fpo}(0)=0,\quad D_{po}\theta_{spo}(0)=0$$

Where $\hat{T}=\dfrac{T_L-T_0}{T_0-T_U}$ specifies the thermal ratio, $\beta=\sqrt{\dfrac{K}{d_{po}{}^2}}$, $\hat{d}=\dfrac{d_{po}}{d_{fl}}$ specifies the depth ratio and $\hat{\mu}=\dfrac{\mu_{po}}{\mu_{fl}}$ specifies the viscosity ratio.

4. Solving using regular perturbation method

At boundaries with constant heat dissipation, convection occurs for smaller horizontal wave number '*a*'. Hence we expand

$$\begin{bmatrix}W_{fl}\\ \theta_{fl}\end{bmatrix}=\sum_{j=0}^{\infty}a_{fl}{}^{2j}\begin{bmatrix}W_{flj}\\ \theta_{flj}\end{bmatrix}\ \text{and}\ \begin{bmatrix}W_{po}\\ \theta_{fpo}\\ \theta_{spo}\end{bmatrix}=\sum_{j=0}^{\infty}a_{po}{}^{2j}\begin{bmatrix}W_{poj}\\ \theta_{fpoj}\\ \theta_{spoj}\end{bmatrix}$$

Zero order system is solved using an arbitrary factor and are

$$W_{fl0}(z_{fl})=0,\ \theta_{fl0}(z_{fl})=\hat{T},\ W_{po0}(z_{po})=0,\ \theta_{fpo0}(z_{po})=1,\ \theta_{spo0}(z_{po})=1$$

The first order equations in $a_{fl}{}^2$ are:

For fluid layer,

$$D_{fl}{}^4W_{fl1}-R_{fl}\hat{T}-Q_{fl}D_{fl}{}^2W_{fl1}=0 \qquad \text{... (27)}$$

$$D_{fl}{}^2\theta_{fl1}-\hat{T}+W_{fl1}=0 \qquad \text{... (28)}$$

For porous layer,

$$D_{po}{}^2W_{po1}+Q_{po}\beta^2D_{po}{}^2W_{po1}+\beta^2R_{Tfpo}+\beta^2R_{Tspo}\tau=0 \qquad \text{... (29)}$$

$$(\phi D_{po}{}^2-H)\theta_{fpo1}+H\theta_{spo1}+W_{po1}-\phi=0 \qquad \text{... (30)}$$

$$[(1-\phi)D_{po}{}^2-H]\theta_{spo1}+H\theta_{fpo1}-(1-\phi)=0 \qquad \text{... (31)}$$

The corresponding boundary conditions are

$$W_{fl1}(1)=0,\quad D_{fl}{}^2W_{fl1}(1)+M_{fl}\theta_{fl0}(1)=0,\quad D_{fl}\theta_{fl1}(1)=0$$

$$\hat{T}W_{fl1}(0)=\hat{d}^2W_{po1}(1),\quad \hat{T}D_{fl}W_{fl1}(0)=\hat{\mu}\hat{d}D_{po}W_{po1}(1)$$

$$\theta_{fl1}(0)=\hat{T}\hat{d}^2\theta_{fpo1}(1),\quad \theta_{fl1}(0)=\hat{T}\hat{d}^2\theta_{spo1}(1)$$

$$D_{fl}\theta_{fl1}(0)=\hat{d}^2D_{po}\theta_{fpo1}(1),\quad D_{fl}\theta_{fl1}(0)=\hat{d}^2D_{po}\theta_{spo1}(1)$$

$$\hat{T}\hat{d}\beta^2D_{fl}{}^3W_{fl1}(0)=-D_{po}W_{po1}(1)+\hat{\mu}\beta^2D_{po}{}^3W_{po1}(1),\quad \hat{T}D_{fl}{}^2W_{fl1}(0)=\hat{\mu}D_{po}{}^2W_{po1}(1)$$

$$W_{po1}(0)=0,\quad D_{po}W_{po1}(0)=0,\quad D_{po}\theta_{fpo1}(0)=0,\quad D_{po}\theta_{spo1}(0)=0$$

W_{fl1} and W_{po1} are obtained by solving equations (27) and (29) and are

$$W_{fl1}(z) = C_1 + C_2 z_{fl} + C_3 \operatorname{Cosh}\sqrt{Q_{fl}}\, z_{fl} + C_4 \operatorname{Sinh}\sqrt{Q_{fl}}\, z_{fl} - \frac{R_{fl}\hat{T}}{2Q_{fl}} z_{fl}^{\,2} \quad \ldots (32)$$

$$W_{po1}(z_{po}) = C_5 + C_6 z_{po} - \frac{\beta^2 R_{Tfpo} + \beta^2 R_{Tspo}\tau}{2(1+Q_{po}\beta^2)} z_{po}^{\,2} \quad \ldots (33)$$

Where the constants C_1, C_2, C_3 ,C_4, C_5 & C_6 evaluated using velocity boundary conditions, are

$$C_1 = \frac{R_{Tfpo} + R_{Tspo}\tau}{\hat{T}(1+Q_{po}\beta^2)}\left[\frac{1}{\hat{d}Q_{fl}} + \hat{\mu}\hat{d}\beta^2\right] - \frac{R_{fl}\hat{T}}{Q_{fl}^{\,2}} + \frac{M_{fl}\hat{T}}{Q_{fl}^{\,2}} + \frac{R_{fl}\hat{T}}{2Q_{fl}}, \quad C_2 = \frac{-(R_{Tfpo} + R_{Tspo}\tau)}{\hat{T}(1+Q_{po}\beta^2)}\left[\frac{1}{\hat{d}Q_{fl}} + \hat{\mu}\hat{d}\beta^2\right],$$

$$C_3 = \frac{R_{fl}\hat{T}}{Q_{fl}^{\,2}\operatorname{Cosh}\sqrt{Q_{fl}}} - \frac{M_{fl}\hat{T}}{Q_{fl}\operatorname{Cosh}\sqrt{Q_{fl}}} - \frac{\operatorname{Tanh}\sqrt{Q_{fl}}}{\hat{T}\hat{d}Q_{fl}\sqrt{Q_{fl}}} \cdot \frac{(R_{Tfpo} + R_{Tspo}\tau)}{1+Q_{po}\beta^2},$$

$$C_4 = \frac{R_{Tfpo} + R_{Tspo}\tau}{1+Q_{po}\beta^2} \cdot \frac{1}{\hat{T}\hat{d}Q_{fl}\sqrt{Q_{fl}}}, \quad C_5 = C_6 = 0$$

4.1 Solvability Condition:

The compatibility condition derived from the differential equations and boundary conditions with respect to temperature is

$$\int_0^1 W_{fl1}(z_{fl})dz_{fl} + \hat{d}^2 \int_0^1 W_{po1}(z_{po})dz_{po} = \hat{d}^2 + \hat{T} \quad \ldots (34)$$

4.2 Solution:

$W_{fl1}(z_{fl})$ & W_{po1} (z_{po}) are substituted in equation (34) and Critical Rayleigh number is attained as

$$R_C = \frac{\hat{d}^2 + \hat{T} - \delta_8}{-\delta_1 + \delta_2 + \delta_3 + \left[\alpha_{FTE}\kappa_{FTD}^{\,2} + \alpha_{STE}\kappa_{STD}^{\,2}\tau\right]\hat{d}^4\Delta_1\left(\delta_4 + \delta_5 - \delta_6 - \delta_7\right)}$$

where $\delta_1 = \frac{\hat{T}}{Q_{fl}^{\,2}}$, $\delta_2 = \frac{\hat{T}}{Q_{fl}^{\,2}\sqrt{Q_{fl}}}\operatorname{Tanh}\sqrt{Q_{fl}}$, $\delta_3 = \frac{\hat{T}}{3Q_{fl}}$, $\delta_4 = \frac{1}{2\hat{T}}\left(\frac{1}{\hat{d}Q_{fl}} + \hat{\mu}\hat{d}\beta^2\right)$,

$$\delta_5 = \frac{1}{\hat{T}\hat{d}Q_{fl}\sqrt{Q_{fl}}}\left[\operatorname{Sinh}\sqrt{Q_{fl}} - \frac{1}{\sqrt{Q_{fl}}}\left(\operatorname{Sech}\sqrt{Q_{fl}} - \operatorname{Cosh}\sqrt{Q_{fl}}\right)\right],$$

$$\delta_6 = \frac{1}{\hat{T}\hat{d}Q_{fl}\sqrt{Q_{fl}}}\left[\operatorname{Sinh}\sqrt{Q_{fl}} - \frac{\operatorname{Cosh}\sqrt{Q_{fl}}}{\sqrt{Q_{fl}}} + \frac{1}{Q_{fl}}\right], \quad \delta_7 = \frac{\hat{d}^2\beta^2}{6}, \quad \delta_8 = \frac{M_{fl}\hat{T}}{Q_{fl}}\left(1 - \frac{\operatorname{Tanh}\sqrt{Q_{fl}}}{\sqrt{Q_{fl}}}\right),$$

$\Delta_1 = \frac{1}{1+Q_{po}\beta^2}$ and $\alpha_{FTE} = \frac{\alpha_{Tfpo}}{\alpha_{Tfl}}$ is the ratio of the thermal expansion coefficients of fluid phase in porous layer to the thermal expansion coefficient in the fluid layer, $\alpha_{STE} = \frac{\alpha_{Tspo}}{\alpha_{Tfl}}$ represents ratio of the thermal expansion coefficient of solid phase in porous layer to the thermal expansion coefficient in the fluid layer, $\kappa_{FTD} = \frac{\kappa_{fl}}{\kappa_{fpo}}$

represents ratio of the thermal in fluid layer to that of solid phase in the porous layer, $\kappa_{STD} = \frac{\kappa_{fl}}{\kappa_{spo}}$ is the ratio of tharmal diffusivity in fluid layer to that of solid phase in the porous layer.

5. Outcomes and discussions

The efficacy of LTNE over the onset of DRBM convection influenced by magnetic field has been analyzed. Comparison of LTE and LTNE models is performed with respect to the critical Rayleigh numbers acquired through regular pertubation technique.

The Critical Rayleigh number R_C against depth ratio $\hat{d}$ for the fixed values of α_{FTE} = 1, κ_{FTD} = 0.4, β = 0.01, $\hat{T}$ =1, Q_{fl} =10 and M_{fl} = 10 has been portrayed graphically. The result on changing each of the variables viz. fluid phase thermal expansion ratio α_{FTE}, fluid phase thermal diffusivity ratio κ_{FTD}, porous parameter β, thermal ratio $\hat{T}$, Chandrasekhar number Q_{fl} and Marangoni number M_{fl} on critical Rayleigh number without altering the remaining parameters with respect to both LTNE & LTE models is presented via Figs.2, 3, 4 and 5, (6) and (7) respectively.

The effects of α_{FTE}, fluid phase thermal expansion ratio on the critical Rayleigh number are displayed in Fig.2. It is observed that the curves are diverging with assigned values α_{FTE} = 1, 5 and 10 which proves that variation effect is protruding in case of composite layer with $d \ll d_m$. It is also evident from the figure that increase in α_{FTE} results into decrease in critical Rayleigh number and hence the set-up can be destabilized. As this parameter augments the vacuity between LTNE and LTE declines and when this parameter is small, the LTNE effects are prominent for larger depth ratios and should be incorporated in the convection problems.

The influence of fluid phase thermal diffusivity ratio κ_{FTD} over critical Rayleigh number are depicted in Fig.3 for κ_{FTD} = 0.1, 0.4 and 0.7. The curves diverge and the observation from the graph is that its effect is to decline in critical Rayleigh number for both LTNE and LTE. Hence the system gets destabilized thereby resulting in early onset of Magneto-DRBM convection. Also as this parameter augments the vacuity between LTNE and LTE diminishes, for smaller values of this parameter, the LTNE effects should not be neglected.

The impact of porous parameter β on critical Rayleigh number are shown in Fig.4. In this case the curves are diverging for values of β = 0.01, 1 and 10 and variation of this parameter, protrudes in case of composite layer with $d \ll d_m$. It is noticed that critical Rayleigh number diminishes when β augments, which is physically reasonable, as there is more window for

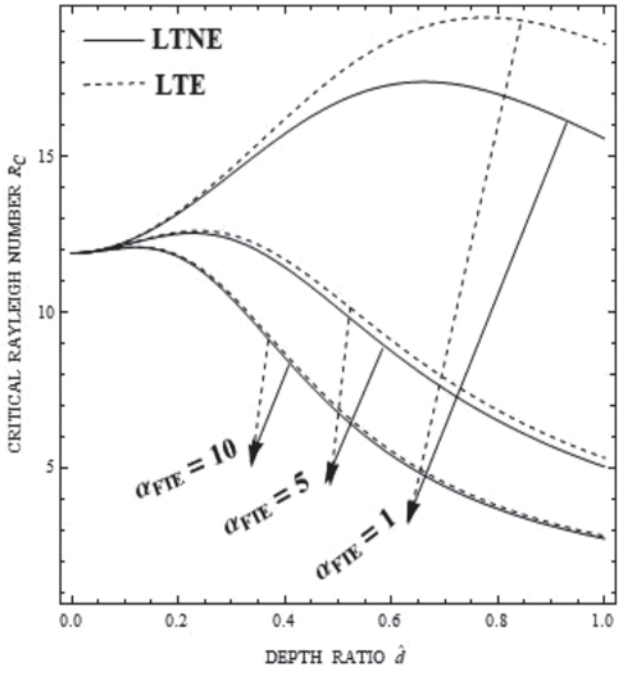

Figure 2

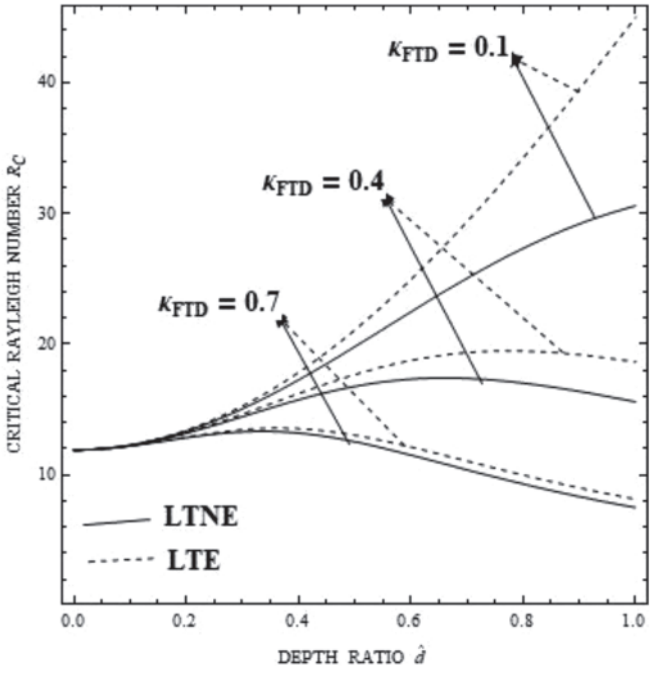

Figure 3

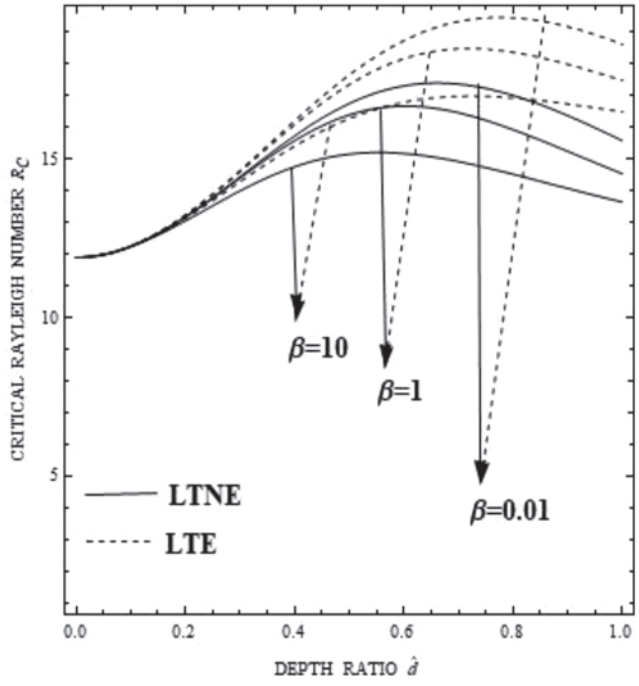

Figure 4

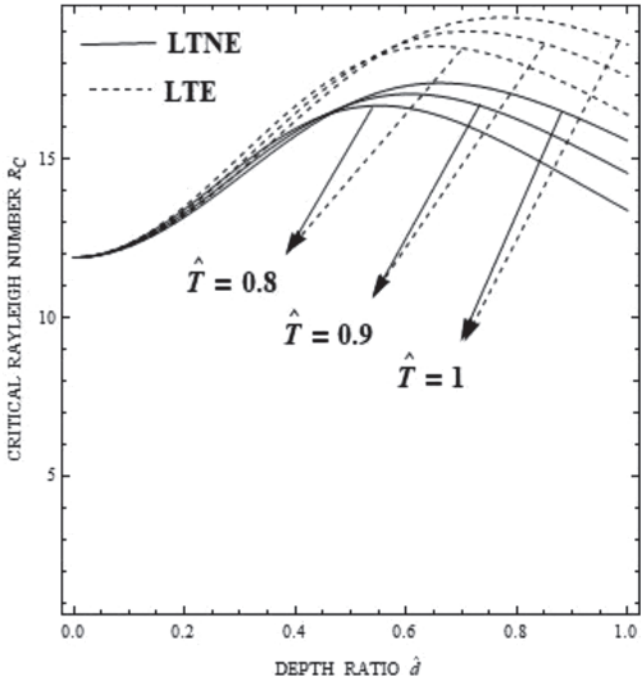

Figure 5

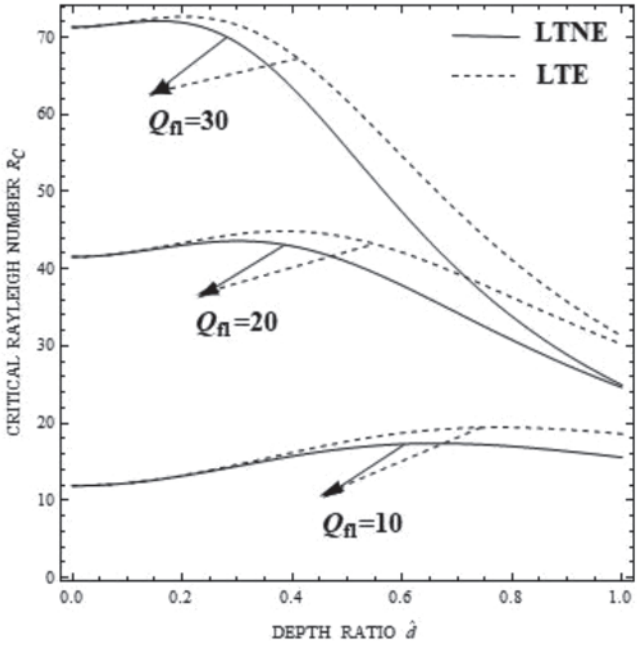

Figure 6

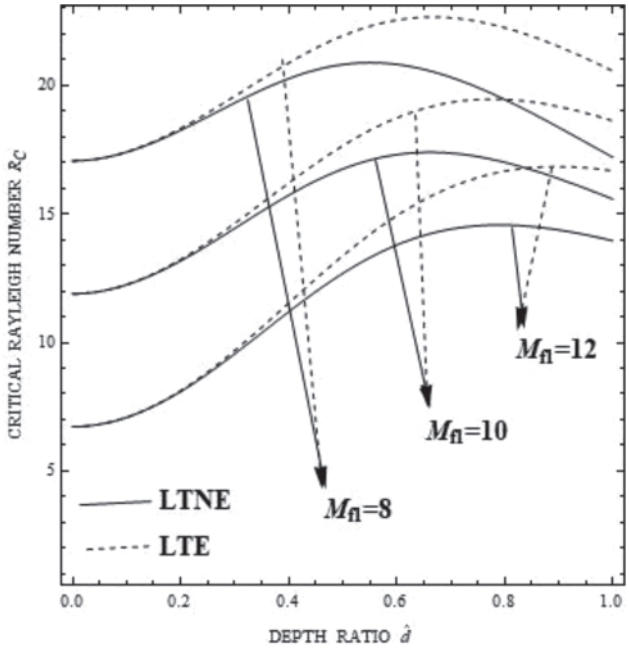

Figure 7

the fluid to move and thereby the system can be destabilised. That is the onset of Magneto-DRBM convection gets preponed.

The effects of thermal ratio $\hat{T}$ over critical Rayleigh number are depicted in Fig.5. In this case, divergene is noticed when $\hat{T}$ = 0.8, 0.9 and 1. The curves diverge, indicating it is sensitive during dominance of porous layer over the composite layer. Increase in critical Rayleigh number is observed when $\hat{T}$ boosts up. Hence the set-up is stable thereby delays the onset of Magneto-DRBM convection.

The influence of Chandrasekhar number Q_{fl} over

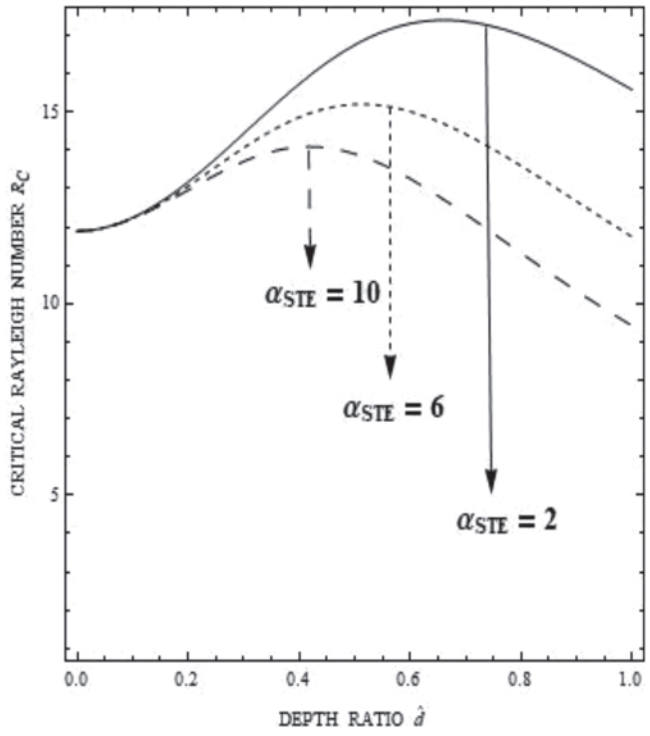

Figure 8

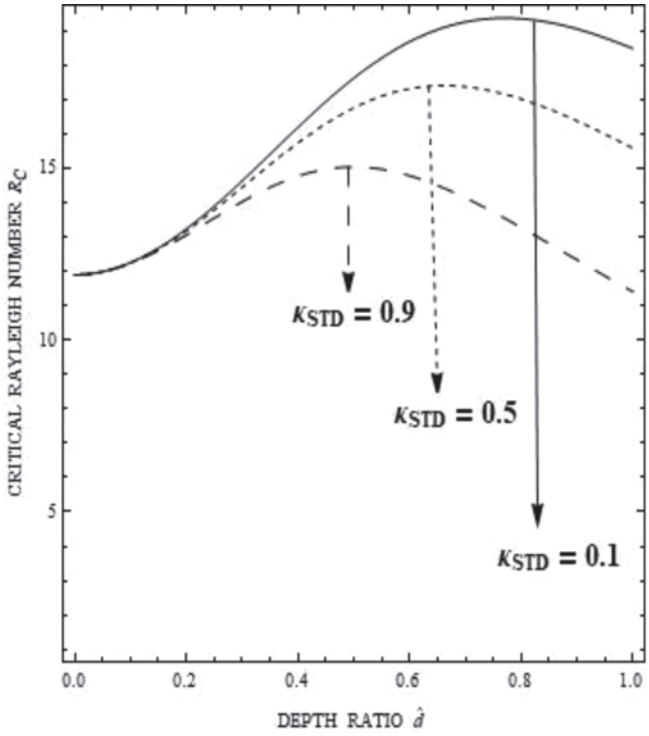

Figure 9

critical Rayleigh number are represented in Fig.6 for Q_{fl} =10, 20, 30. In this case the curves are converging for higher values of Q_{fl}. Indicating that it is sensitive for fluid layer dominant composite layer. Also, augmentation in Q_{fl} raises the critical Rayleigh number value thereby stabilizing the system. Hence the onset of DRBM convection gets postponed in the presence of magnetic field.

The effects of Marangoni number M_{fl} over critical Rayleigh number are displayed in Fig.7. In this case, slight convergence of the curves is noticed for values of M_{fl} = 8, 10 and 12. Observation through the graph is that critical Rayleigh number boosts up when M_{fl} declines. Hence the set-up is unstable which allows quicker onset of Magneto-DRBM convection for both LTNE and LTE.

Parameters influencing LTNE specifically are, nothing but solid phase thermal expansion ratio a_{STE}, solid phase thermal diffusivity ratio k_{STD} and inter-phase thermal diffusivity ratio t. Figs.8, 9 and 10 depict the effect of these parameters on critical Rayleigh number keeping the other parameters fixed as mentioned above.

The effects of solid phase thermal expansion ratio a_{STE} over critical Rayleigh number are represented in figure (8) considering a_{STE} = 2, 6 and 10. The curves are found diverging showing that it is sensitive when composite

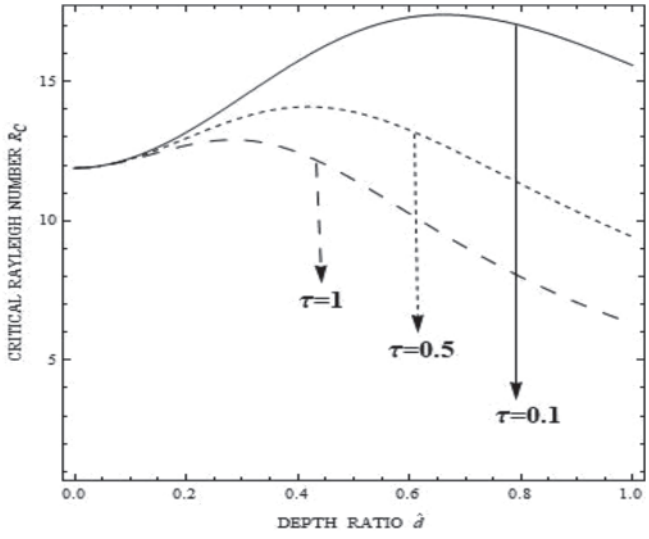

Figure 10

layer is dominated by porous layer, which is, as expected. Study reveals that the critical Rayleigh number diminishes when a_{STE} augments which destabilizes the system. Hence, there is quicker onset of Magneto-DRBM convection.

The influence of solid phase thermal diffusivity ratio k_{STD} over critical Rayleigh number are depicted in Fig.(9) when k_{STD} = 0.1, 0.5 and 0.9. Divergence is noticed from the figure and is evident that it is

sensitive in composite layers dominated by porous layer. Also, decline in critical Rayleigh number is noticed when κ_{STD} rises which destabilizes the system. Hence, onset of Magneto-DRBM convection is preponed.

The impact of inter-phase thermal diffusivity ratio τ over critical Rayleigh number are displayed in figure (10) for $\tau = 0.1$, 0.5 and 1. The diverging curves indicate the sensitiveness of this parameter for the porous layer dominant composite layers. The study reveals that the critical Rayleigh number dimishess when τ augments thereby destabilizing the set-up. Hence onset of Magneto-DRBM convection occurs quickly.

Conclusions

i. The critical Rayleigh numbers for LTE are higher than the same for LTNE model. The convection sets in earlier due to LTNE effects. The LTNE effects cannot be neglected in the case of situations where convection has to be controlled.
ii. Fluid phase thermal expansion ratio, fluid phase thermal diffusivity ratio porous parameter and Marangoni number boost the early onset of Magneto-DRBM convection in composite systems dominanted by porous layer for both LTNE and LTE models.
iii. Thermal ratio and Chandrasekhar number postpones the onset of Magneto- DRBM convection. Dominance of thermal ratio is protrusive in composite systems dominanted by porous layer for both LTNE and LTE models whereas Chandrasekhar number is effectual in fluid layer dominant composite set-up.
iv. For any composite layer systems, one can control the onset of Magneto-DRBM convection by choosing values of thermal ratio and Chandrasekhar number for both LTNE and LTE models.
v. Thermal diffusivity ratio with respect to fluid phase and solid phase as well as inter-phase thermal diffusivity ratio are parameters pertaining to LTNE which guarantee the quicker onset of Magneto-DRBM convection.

References

[1] Jyoti Ahuja, Magneto convection for a nanofluid layer with local thermal non-equilibrium (LTNE) model: A realistic approach, Materials Today: Proceedings, Volume 26, Part 3, 2020, Pages 3407-3415, https://doi.org/10.1016/j.matpr.2019.11.112, (2019).

[2] Mehryan S.A.M, Mohsen Izadi, Mikhail A.Sheremet, Analysis of conjugate natural convection within a porous square enclosure occupied with micropolar nanofluid using local thermal non- equilibrium model, Journal of Molecular Liquids, Volume 250, Pages 353-368, (2018).

[3] Min Zeng, Qiu-Wang Wang, Zi-Peng Huang, Gang Wang, and Hiroyuki Ozoe, Numerical investigation of natural convection in an enclosure filled with porous medium under magnetic field, Numerical Heat Transfer, Part A, 52: 959–971, (2007).

[4] Min Zeng, Qiuwang Wang, Hiroyuki Ozoe, Gang Wang and Zipeng Huang, Natural convection of diamagnetic fluid in an enclosure filled with porous medium under magnetic field, Progress in Computational Fluid Dynamics, Vol. 9, No. 2, (2009).

[5] Mohsen Izadi, Rasul Mohebbi , Hasan Sajjadi , Amin Amiri Delouei, LTNE modeling of Magneto-Ferro natural convection inside a porous enclosure exposed to nonuniform magnetic field, Physica A 535 (2019) 122394.

[6] Mohsan Hassan, Measurement of Heat and Mass Flow Characteristics of Nanofluid in a Porous Parallel-Plate Channel by Darcy-LTNE/LTE, Brinkman-LTNE/LTE Models, Open access peer-reviewed chapter, DOI: http://dx.doi.org/10.5772/intechopen.83482, (2019).

[7] Phadungsak Rattanadecho and Waraporn Klinbun, Numerical Analysis of Natural Convection in Porous Media Subjected to Electromagnetic Energy Using Local Thermal Nonequilibrium (LTNE) Models, Drying Technology, 30: 1896–1905, ISSN: 0737-3937 print/1532-2300 online, (2012).

[8] Pouya Barnoon, Davood Toghraie, Mohammad Salarnia and Arash Karimipour, Mixed thermomagnetic convection of ferrofuid in a porous cavity equipped with rotating cylinders: LTE and LTNE models, Journal of Thermal Analysis and Calorimetry, https://doi.org/10.1007/s10973-020-09866-7, (2020).

[9] Puneet Rana, Meenakshi Khurana, LTNE thermoconvective instability in Newtonian rotating layer under magnetic feld utilizing nanoparticles, Journal of Thermal Analysis and Calorimetry, https://doi.org/10.1007/s10973-020-10301-0, (2020).

[10] Ravisha M, I.S. Shivakumara, Mamatha A.L, Cattaneo–LTNE porous ferroconvection, Multidiscipline Modeling in Materials and Structures, DOI: 10.1108/MMMS-11-2018-0189, (2019).

[11] Srivastava A. K and B. S. Bhadauria, Influence of Magnetic Field on Fingering Instability in a Porous Medium with Cross-Diffusion Effect: a Thermal Non-equilibrium Approach, Journal of Applied Fluid Mechanics, Vol. 9, No. 6, pp. 2845-2853, ISSN 1735-3572, EISSN 1735-3645, (2016).

[12] Sumithra R and N. Manjunatha, Effects of Heat Source/ Sink and non-uniform temperature gradients on Darcian-Benard-Magneto-Marangoni convection in ' composite layer horizontally enclosed by adiabatic boundaries, Malaya Journal of Matematik, Vol. 8, No. 2, 373-382, (2020).

[13] Zargartalebia Hossein, Mohammad Ghalambaz, Aminreza Noghrehabadi and Ali. J. Chamkha, Natural convection of a nanofluid in an enclosure with an inclined local thermal non-equilibrium porous fin considering Buongiorno's model, NUMERICAL HEAT TRANSFER, PART A 2016, VOL. 70, NO. 4, 432–445 http://dx.doi.org/10.1080/10407782.2016.1173483, (2016).